

Physiological and Biochemical Characterization of AnNitA, the *Aspergillus nidulans* High-Affinity Nitrite Transporter

Shiela E. Unkles, Vicki F. Symington, Zorica Kotur, Ye Wang, M. Yaeesh Siddiqi, James R. Kinghorn and Anthony D. M. Glass

Eukaryotic Cell 2011, 10(12):1724. DOI:
10.1128/EC.05199-11.

Published Ahead of Print 21 October 2011.

Updated information and services can be found at:
<http://ec.asm.org/content/10/12/1724>

These include:

REFERENCES

This article cites 39 articles, 11 of which can be accessed free at: <http://ec.asm.org/content/10/12/1724#ref-list-1>

CONTENT ALERTS

Receive: RSS Feeds, eTOCs, free email alerts (when new articles cite this article), [more»](#)

Information about commercial reprint orders: <http://journals.asm.org/site/misc/reprints.xhtml>
To subscribe to to another ASM Journal go to: <http://journals.asm.org/site/subscriptions/>

Physiological and Biochemical Characterization of AnNitA, the *Aspergillus nidulans* High-Affinity Nitrite Transporter[∇]

Shiela E. Unkles,¹ Vicki F. Symington,¹ Zorica Kotur,² Ye Wang,² M. Yaesh Siddiqi,²
James R. Kinghorn,¹ and Anthony D. M. Glass^{2*}

School of Biology, University of St. Andrews, St. Andrews, Fife KY16 9TH, United Kingdom,¹ and Department of Botany, University of British Columbia, Vancouver, British Columbia V6T 1Z4, Canada²

Received 20 August 2011/Accepted 12 October 2011

High-affinity nitrite influx into mycelia of *Aspergillus nidulans* has been characterized by use of ¹³NO₂⁻, giving average *K_m* and *V_{max}* values of 48 ± 8 μM and 228 ± 49 nmol mg⁻¹ dry weight (DW) h⁻¹, respectively. Kinetic analysis of a plot that included an additional large number of low-concentration fluxes gave an excellent monophasic fit (*r*² = 0.96), with no indication of sigmoidal kinetics. Two-dimensional (2D) and three-dimensional (3D) models of AnNitA are presented, and the possible roles of conserved asparagine residues N122 (transmembrane domain 3 [Tm 3]), N173 (Tm 4), N214 (Tm 5), and N246 (Tm 6) are discussed.

Although nitrate and ammonium are the major sources of nitrogen for bacteria, fungi, algae, and plants, nitrite may also represent a significant nitrogen source under some circumstances. For example, in waterlogged anaerobic soils as well as in aerobic soils where gaseous anaerobic pockets exist, substantial levels of nitrite may accumulate (14). Phytoplankton has been shown to excrete significant amounts of nitrite when nitrate uptake exceeds the capacity for the assimilation of the nitrite generated (20). Conditions such as low light, low temperature, or a disruption of the nitrate reductase activity (40) may result in nitrite efflux that matches nitrate uptake in a 1:1 stoichiometry. This nitrite may subsequently be taken up and converted to ammonium by assimilatory nitrite reductase, followed by assimilation into organic nitrogenous compounds within root plastids or chloroplasts (2). As well as being a source of nitrogen for a range of organisms, there are associated agricultural, environmental, and even medical issues involved in nitrite biogeochemistry (16, 37).

There is a substantial amount of information available for the nitrite assimilatory enzyme system, nitrite reductase, as well as certain nitrate uptake systems that also transport nitrite as well as nitrate. These bispecific permeases (together with those that transport nitrate only, such as *Chlamydomonas reinhardtii* NRT2.2) are characterized by 12 transmembrane α-helical domains (Tms), a nitrate signature, and a major facilitator superfamily (MFS) motif and belong to the nitrate NNP (nitrate nitrite porter) subgroup (TC 2.A.1) of the MFS (21, 25, 33).

In contrast, there are transporters that transport nitrite but not nitrate, for which much less is known. These transporters include *Escherichia coli* EcNirC (3, 12, 13), *Aspergillus nidulans* AnNitA (40), and *C. reinhardtii* CrNar1, which possesses no fewer than six paralogs (18, 23). Such proteins belong to a family quite separate from the MFS, known as the formate/

nitrite transporter (FNT) family (TC 2.A.44), and many FNT members are thought to transport nitrite and/or the structurally related formate. FNT family members are found in the microbial kingdoms of archaea, eubacteria, protista, and fungi. Most members of the FNT family probably possess 6 Tms and are much smaller (at the primary protein sequence level) than NNP proteins. For example, the *A. nidulans* AnNitA protein possesses 310 amino acid residues, compared to the AnNrtA high-affinity nitrate transporter, which has 507 amino acid residues. Recently, a structural analysis of the purified FocA proteins (members of the FNT family) from *E. coli* (7, 41) and *Vibrio cholerae* (38) suggested that these proteins are pentameric formate channels, with each FocA subunit being made up of six transmembrane α-helices. FocA channels, with affinities for formate that may be in the millimolar to tens of millimolar range (38), are thought to export formate generated from pyruvate during anaerobic respiration. The extent of cooperativity among subunits and the nature of the true substrate(s), formate or nitrite, still remain unresolved. Despite the recognition from genome sequence data that a large family of orthologous FNT proteins is distributed among a wide range of microorganisms, little detailed information is available on the mechanism of action of these proteins. Previous evidence of the six-Tm topology of this group has come from the *E. coli* EcFocA protein, characterized as a formate transporter on the basis of the resistance of transposon insertion mutants to the formate analog hypophosphite (30). Subsequent studies of deletion mutants have demonstrated that *E. coli* EcNirC transports nitrite (3), as does at least one of the *C. reinhardtii* paralogs, the chloroplast membrane-localized CrNar1.1 protein (23). Electrophysiological studies showed that the *C. reinhardtii* CrNar1.2 chloroplast membrane-located protein appears to be a high-affinity nitrite and low-affinity carbonate transporter (18). A putative chloroplast nitrite transporter, CsNir1-L, has also been identified in cucumber (28).

Until recently, there was no information regarding amino acid residues within FNT proteins that might be important for the nitrite transport function. However, three crystal structures of FNT proteins have now been solved, all of which are formate channels: *E. coli* EcFocA (41), *Vibrio cholerae* VcFocA

* Corresponding author. Mailing address: Department of Botany, University of British Columbia, Vancouver, British Columbia V6T 1Z4, Canada. Phone: (604) 822-4847. Fax: (604) 822-6089. E-mail: anthonyd.glass@botany.ubc.ca.

[∇] Published ahead of print on 21 October 2011.

(38), and *Salmonella enterica* serovar Typhimurium StFocA (15). These structures have allowed the development of a model for the AnNitA protein. Perhaps surprisingly, given that NNP and certain FNT proteins share the same substrate, nitrite, the crucial conserved arginine residues that bind nitrate in NNP proteins (35) are not present in the FNT group of transporters.

Previous $^{13}\text{NO}_3^-$ tracer studies showed that wild-type strains of *A. nidulans* possess two high-affinity nitrate transporters (NrtA and NrtB) that, in common with high-affinity nitrate transporters from other organisms (8), also transport nitrite (40). Mutant strains lacking NrtA and NrtB showed no $^{13}\text{NO}_3^-$ tracer uptake yet are capable of growth on nitrite and a net uptake of nitrite (40). Our previous studies included obtaining accurate K_m and V_{\max} values using ^{13}N -nitrate influx for the *A. nidulans* NrtA and NrtB nitrate transporters (36). In this article, we extended this line of study by generating the short-lived tracer ^{13}N -nitrite for nitrite transport studies. Such tracer experiments permit a more accurate determination of kinetic constants than can be obtained by use of assays of net nitrite uptake. In addition, results of *in vitro* mutational studies of AnNitA residues, highly conserved in FNT proteins, as well as the oligomeric state of the protein are presented.

MATERIALS AND METHODS

***Escherichia coli* strains, plasmids, and media.** Standard procedures were used for the propagation of plasmids as well as for the subcloning and maintenance of plasmids within *E. coli* strain DH5 α .

Fungal strains. *A. nidulans* strains used in this study and described previously (40) are double deletion mutant strain T110 (*nrtA747 nrtB110*) (disrupted in both the *nrtA* and *nrtB* genes), which has wild-type AnNitA without the V5 tag, used as the negative control for the Western blots, and triple deletion mutant strain T26 (*nrtA747 nrtB110 nitA26*) (disrupted in the *nrtA*, *nrtB*, and *nitA* genes), used for kinetic studies. Strains generated for this study were double deletion transformant strains T600 and T5275 (disrupted in both the *nrtA* and *nrtB* genes as described above), which have wild-type AnNitA with the V5 tag, used for kinetic studies and Western blots; strain T454, expressing V5-tagged, nitrate/nitrite transporter AnNrtA for Western analyses; and strain VFS106 (*nrtA747 nrtB110 argB2 nkuA::argB* pyroA2*), used as the recipient to facilitate high-throughput transformation as well as to ensure crossover and integration at the *nitA* locus.

Fungal growth media and handling techniques. Fungal growth media and handling techniques were described previously (4). Shake flask cultures for nitrate uptake assays were grown in liquid minimal medium (5).

Generation of NitA amino acid replacement constructs. For the generation of mutations by PCR overlap extension (42), the template was plasmid pV5MKNITA, which comprises the *nitA* coding region to which a sequence encoding the V5 epitope (Invitrogen) was fused in frame at the 3' end. Following the stop codon is 300 bp of the *nrtA* terminator. Details of primers used for mutagenesis are available from the authors. Mutant fragments were inserted into pV5MKNITA using unique restriction sites. Following cloning, all DNA fragments generated by PCR amplification were sequenced to verify the existence of the desired mutation and the absence of other PCR-induced mutations. PCR fragments for transformation were generated by the primary amplification of four overlapping fragments—500 bp of sequence directly upstream from the *nitA* start codon; the coding region, including the V5 tag and *nrtA* terminator; the *Aspergillus fumigatus pyroA* gene; and 1 kb of the region downstream from *nitA*—followed by a PCR fusion reaction to create the final product incorporating the four primary fragments (31).

Fungal genetic transformation procedure and selection of transformants. The *A. nidulans* transformation procedure used was essentially that carried out as described previously (see reference 24 and references therein). The selection of transformants was based on the pyridoxine prototrophy of strain VFS106 following transformation with fusion PCR fragments containing the *nitA* mutant sequence and the *A. fumigatus pyroA* gene for selection. Transformants (*pyroA*⁺) were screened for the utilization of 2 mM nitrite as the sole source of nitrogen. Growth was assessed after (i) 2 days at 37°C and (ii) 4 days at 25°C to determine if the mutation resulted in temperature sensitivity or cryosensitivity.

Molecular analyses of fungal transformants. With the selection system used, *pyroA*⁺ transformants normally contain a single copy at the resident *nitA* locus, but location and copy number were nevertheless verified by Southern hybridization. The conditions used during Southern analysis were described previously (34). Finally, the entire DNA sequence of the *nitA* coding region in mutant transformants was determined by automated sequence analysis as described previously (34).

Synthesis of the ^{13}N -nitrite tracer. ^{13}N -nitrate was generated by proton irradiation of water at the cyclotron facility (Tri-University Meson Facility), University of British Columbia, as described previously (36). This radioactive nitrate was used as the source material to generate ^{13}N -nitrite according to a method described previously by McElfresh and colleagues (19). Trace quantities of hydrogen peroxide, added to the irradiated water to promote an oxidizing environment, were removed by the addition of a commercial catalase enzyme, since the reduction of nitrate to nitrite by a cadmium column was compromised by the presence of hydrogen peroxide. Nitrate-13 was then passed twice through the column prepared according to methods described previously by McElfresh and colleagues (19). This procedure generated >96% ^{13}N -nitrite, as determined by passing the column eluate through a high-performance liquid chromatograph (HPLC) with a gamma detector in series with the column. Passage through the column resulted in the replacement of the nitrate-13 peak by a peak corresponding to nitrite-13. After the cadmium reduction, the column eluate was treated with 2 N KOH and boiled for 2 min to remove any contaminating NH_4^+ .

Fungal uptake assays with ^{13}N -nitrite. The growth of strains and assay of nitrite influx at the standard concentration range for high-affinity transport (10 to 250 μM) were detailed for ^{13}N -nitrate in our previous report (36). Briefly, strains were grown for a total of 7 h at 37°C in minimal medium containing 5 mM urea, to which 5 mM potassium nitrite was added to induce the nitrate assimilation pathway 3 h prior to harvesting. Following harvesting by filtration and washing to remove nitrite, fungi were resuspended in fresh nitrogen-free minimal medium contained in 250-ml Erlenmeyer flasks. The flasks were shaken in a water bath at 37°C and inoculated with appropriate volumes of a freshly prepared 10 mM stock of potassium nitrite solution to bring the medium to the desired concentration, and an aliquot of the $^{13}\text{NO}_2^-$ stock was added immediately (negligible nitrite concentration). After 5 min of incubation (transport is linear for at least 30 min), five 10-ml aliquots were filtered individually through glass fiber filters and washed twice with 200 ml of 200 μM nitrite to remove the unabsorbed tracer. This procedure has been shown to remove all but negligible traces of ^{13}N from mycelia and filters. Each filter was introduced into a plastic scintillation vial, and the accumulated radioactivity was determined by gamma counting with a Canberra Packard gamma counter. Values for influx are expressed as nmol nitrite per mg of dry weight (DW) of mycelium per hour. Normally, each K_m or V_{\max} value was determined by linear regression of a Hoffstee analysis (a plot of V against V/S) and by a direct hyperbolic fit, with five replicates at each of the seven concentrations used. For each transformant, a completely independent experiment was run twice; results were highly reproducible. In order to explore the possibility of sigmoidal kinetics associated with AnNitA activity at low external nitrite concentrations, 6 additional concentrations of nitrite (7.5, 5, 2.5, 1, 0.5, and 0.25 μM) were used to measure nitrite influx in strains containing only the wild-type AnNitA protein (namely, T600, an *nrtA nrtB* double deletion strain).

Q_{10} determinations. Q_{10} determinations were performed by incubating strains T600 and T26 in standard uptake medium containing 100 μM KNO_2 at 10°C and 23°C. The net uptake of nitrite was determined after 15 min, and Q_{10} values were calculated from the equation $Q_{10} = (R_2/R_1)^{10/(T_2 - T_1)}$, where R_1 and R_2 are uptake rates at 10°C (temperature 1 [T₁]) and 23°C (T₂). Detailed protocols describing net nitrite uptake were reported previously (40).

Formate-nitrite interactions. To investigate whether NitA might also transport formate, we undertook classic substrate competition studies. Maintaining a constant nitrite concentration of 100 μM KNO_2 , formate was added at 100, 200, and 500 μM in medium buffered at pH 6.0. Nitrite uptake was then determined for strain T600 (expressing NitA) according to standard protocols. Additionally, using [^{14}C]formate, we measured formate uptake by T600 and T26 (disrupted in NitA).

NitA protein purification from *Pichia pastoris*. The *A. nidulans nitA* gene, with a sequence encoding an N-terminal six-histidine tag and a tobacco etch virus (TEV) protease recognition site, was expressed by using the *Pichia pastoris aox* promoter and terminator following transformation and selection using phleomycin resistance as a selectable marker (1). *P. pastoris* cells were grown for 24 h in yeast extract-peptone-dextrose (YPD) medium and transferred into minimal medium containing 0.5% methanol for 24 h before harvesting. Cells were disrupted at 30 lb/in² by use of a Constant cell disruption system (Constant Systems Ltd., Daventry, United Kingdom), cell debris was removed by centrifugation at 2,500 \times g for 15 min at 4°C, and crude membranes were pelleted by centrifuga-

tion at $25,000 \times g$ for 45 min at 4°C . Membranes were solubilized in 1% dodecyl- β -D-maltoside (DDM; Anatrace), and the NitA protein was purified with Talon metal affinity chromatography resin (BD Biosciences), during which the detergent concentration was reduced to 0.016%. The histidine tag was excised by incubation with TEV protease (Invitrogen), and the tag was removed by a second run through Talon resin, collecting purified AnNitA protein in the flowthrough.

Western blots of *A. nidulans* membrane proteins. Strains were grown for around 5 h in 400 ml minimal medium at 37°C with 5 mM urea as the sole nitrogen source and induced with 10 mM sodium nitrite for a further 3 h. Cells were harvested by filtration through sterile Myra cloth (Calbiochem, EMD Biosciences) and washed with cold sterile distilled water. Mycelia (pressed wet weight of 300 mg) were ground in liquid nitrogen, with the powder being resuspended in 10 ml extraction buffer (20 mM Tris [pH 7.5] at 4°C , 100 mM 6-amino hexanoic acid, 5% [vol/vol] glycerol, 1 mM benzamidine). Crude plasma membrane suspensions were made by the centrifugation of fungal suspensions at $2,500 \times g$ for 15 min at 4°C , followed by the centrifugation of the supernatant at $25,000 \times g$ for 45 min at 4°C . The gelatinous pellet was resuspended in 80 μl of extraction buffer and stored at -85°C . Protein concentration estimations were made by using a BCA protein assay kit (Pierce). Following the solubilization of membranes in 1% DDM, 50 μg of protein was electrophoresed by blue native polyacrylamide gel electrophoresis (BN-PAGE) on 4-to-17% gradient gels according to a method described previously (11). Western blotting of the gel was performed according to standard protocols, with the additional step of a destaining of the polyvinylidene difluoride (PVDF) membrane with PAGE destain (45% [vol/vol] ethanol, 10% [vol/vol] acetic acid) for 10 min prior to blocking. Standard size markers (bovine serum albumin, rabbit muscle lactate dehydrogenase, equine spleen ferritin, and porcine thyroid thyroglobulin; all from Sigma) were run alongside the extracted proteins. Immunological detection was carried out by use of horseradish peroxidase (HRP)-conjugated anti-V5 antibody (Invitrogen) and visualized with enhanced chemiluminescent reagents (GE Healthcare). Blots were washed in stripping buffer (100 mM β -mercaptoethanol, 2% SDS, 62.5 mM Tris-HCl [pH 6.7]) at 60°C for 30 min with occasional agitation before immunodetection was repeated by using an antibody to the *Saccharomyces cerevisiae* H^{+} -ATPase Pma1 (Santa Cruz Biotechnology) to demonstrate the approximate equality of protein loading and transfer.

Generation of 2D and 3D models of AnNitA. The alignment of protein sequences was carried out by using ClustalW (32). Models were generated by using the Bioinformatics Toolkit (<http://toolkit.tuebingen.mpg.de>). Alignments of structural homologs were made by using HHpred (27), and a three-dimensional (3D) model was created by using Modeller (26) based on EcFocA (Protein Data Bank [PDB] accession number 3KCU). The N-terminal 28 residues and the C-terminal 45 residues were not included in the two-dimensional (2D) or 3D models. 3D figures were generated by using Pymol (6).

RESULTS

Effect of pH on ^{13}N -nitrite tracer accumulation in a strain disrupted in the *nrtA*, *nrtB*, and *nitA* genes. We followed procedures detailed previously (19) to generate the short-lived tracer ^{13}N -nitrite for nitrite influx experiments to permit a more accurate determination of kinetic constants than can be obtained with nonradioactive net nitrite (^{14}N -nitrite) transport assays (see Materials and Methods for more details). The use of HPLC established that a $>96\%$ conversion of ^{13}N -nitrate to ^{13}N -nitrite was achieved, with no ^{13}N -ammonium present. To investigate the possibility of nitrous acid (HNO_2) permeation, ^{13}N -nitrite influx was determined for strain T26 (carrying *nrtA747*, *nrtB110*, and *nitA26* mutations). Since this strain lacks nitrate and nitrite transporters, any ^{13}N accumulation would represent the passive permeation of $^{13}\text{NO}_2^-$ or H^{13}NO_2 . We manipulated the speciation of $^{13}\text{NO}_2^-/\text{H}^{13}\text{NO}_2$ by varying the pH from pH 3.5 (close to the pK_a of nitrous acid) to pH 8.5 and measured ^{13}N accumulation in T26 using a 250 μM external nitrite concentration (Fig. 1). The optimum pH for the influx of nitrous acid occurred at pH 3.5 and declined as the pH increased.

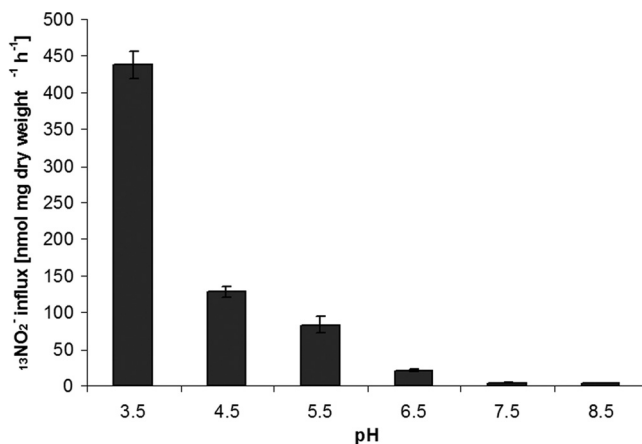


FIG. 1. ^{13}N -nitrite influx in strain T26 (*nrtA747 nrtB110 nitA26*) to evaluate the extent of nitrous acid (HNO_2) permeation at various pH values. The nitrite concentration was 250 μM .

Influx of ^{13}N -nitrite by NitA. The use of a radioactive tracer has numerous advantages over net nitrite (^{14}N -nitrite) depletion studies. There is clear evidence (see the introduction) that nitrite efflux, either due to the activity of the nitrate/nitrite transporters or by a separate nitrite efflux system, can be substantial. Hence, net measurements of ^{14}N -nitrite uptake may be compromised by simultaneous efflux. By using short-term measurements of a 5-min duration with ^{13}N -nitrite, we are able to characterize the influx activity of AnNitA, and the sensitivity of gamma detection permitted influx measurements even at nanomolar concentrations. In the present study, V_{max} and K_m values for the wild-type AnNitA protein (using strain T600, carrying the *nrtA747* and *nrtB110* mutations) were determined by means of Hoffstee analysis, which gave average values (based upon 8 separate experiments) of 228 ± 49 nmol mg^{-1} DW h^{-1} and 48 ± 8 μM , respectively. The Hoffstee plot gave an excellent monophasic fit ($r^2 = 0.93$). In the current study, strain T600 (expressing wild-type AnNitA in the *nrtA747 nrtB110* double deletion mutant background) was used to eliminate nitrite being taken up by the bispecific permeases AnNrtA and AnNrtB. In order to explore for the presence of sigmoidal kinetics, Fig. 2A includes influx data, using strain T600, at six low concentrations of ^{13}N -nitrite (7.5, 5, 2.5, 1, 0.5, and 0.25 μM), in addition to a standard concentration range (10 to 250 μM). Sigmoidal kinetics are typical of allosteric enzymes exhibiting cooperativity among subunits. These data gave V_{max} and K_m values of 214 ± 8 nmol mg^{-1} DW h^{-1} and 35 ± 4 μM , respectively, using a direct hyperbolic fit and 212 ± 11 nmol mg^{-1} DW h^{-1} and 35 ± 2.5 μM , respectively, using Hoffstee analysis. In contrast, strain T26 (*nrtA747 nrtB110 nitA26* triple deletion mutant) showed linear kinetics, with very low levels of nitrite influx (Fig. 2A). For example, at 100 μM , the rate of nitrite influx in T26 averaged 22 nmol mg^{-1} DW h^{-1} , compared to 142 nmol mg^{-1} DW h^{-1} for T600. Hyperbolic kinetics were restored to strain T26 ($V_{\text{max}} = 162 \pm 14$ nmol mg^{-1} DW h^{-1} and $K_m = 41 \pm 7$ μM) when it was transformed with the wild-type *nitA* gene to generate strain T5275 (Fig. 2B). The metabolic dependence of nitrate uptake was revealed through Q_{10} (temperature coefficient) experiments, which resulted in values of 1.82 ± 0.02 and 1.06 ± 0.05

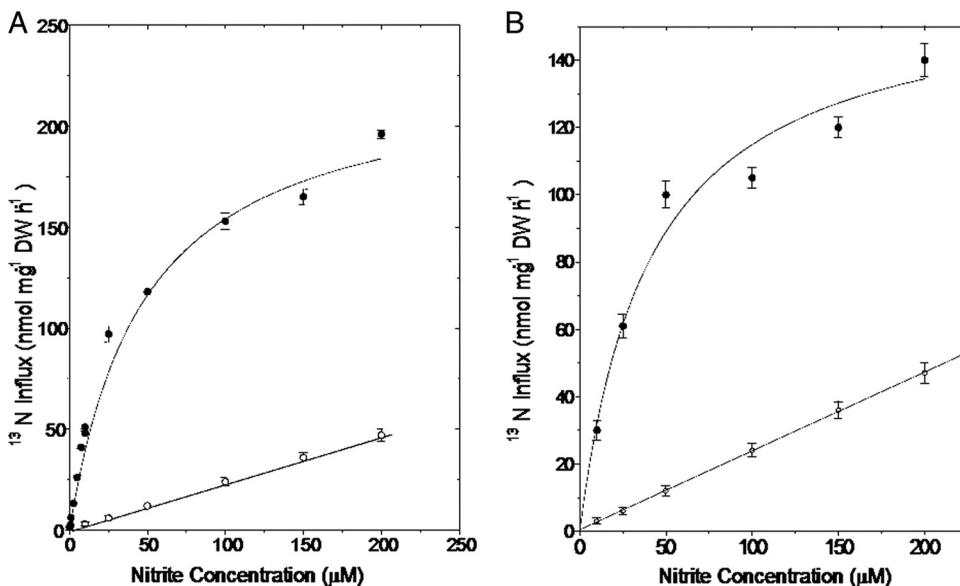


FIG. 2. Concentration dependence of ¹³NO₂⁻ influx. (A) ¹³N-nitrite influx (nmol mg⁻¹ DW h⁻¹) in T600 (*nrtA747 nrtB110*) (●), expressing AnNitA, and in T26 (*nrtA747 nrtB110 nitA26*) (○), lacking AnNitA. Hoffstee analysis (*r*² = 0.95) gave *V*_{max} and *K*_m values of 212 ± 11 nmol mg⁻¹ DW h⁻¹ and 35 ± 2.5 µM, respectively, for T600. Linear regression of T26 data gave an *r*² of 0.999. (B) ¹³N-nitrite influx (nmol mg⁻¹ DW h⁻¹) in strain T26 (*nrtA747 nrtB110 nitA26*) (○) and in T26 after a knock-in transformation with the wild-type *nitA* gene to give strain T5275 (●). Hoffstee analysis (*r*² = 0.93) gave *V*_{max} and *K*_m values of 162 ± 14 nmol mg⁻¹ DW h⁻¹ and 41 ± 7 µM, respectively, for strain T5275. Linear regression of T26 gave an *r*² of 0.94.

for strains T600 and T26, respectively, at temperatures of 10°C and 23°C. Typically, Q₁₀ values significantly greater than 1 characterize metabolic processes. The incubation of strain T600 in the presence of 100, 200, and 500 µM formate showed no reduction of NO₂⁻ uptake (data not shown). The [¹⁴C]formate uptake by strain T26 (with disrupted *NitA*) was not reduced (data not shown) compared to that by T600 (expressing *NitA*).

NitA protein isolation. Milligram quantities of pure AnNitA protein were made from the yeast *P. pastoris*, which was used as the AnNitA expression host (see Materials and Methods), and AnNitA protein identity and integrity were verified by mass spectrometry (data not shown). Blue native polyacrylamide gel electrophoresis (BN-PAGE) was used to investigate the quaternary structure of AnNitA according to a method described previously (11) for membrane proteins. This approach takes into account the contribution of bound detergent and Coomassie brilliant blue dye to the observed mass. In comparison to standard proteins, AnNitA showed an apparent molecular mass of 230 kDa by BN-PAGE, which is equivalent to an actual mass of around 128 kDa (Fig. 3). Upon prior treatment with 1% SDS, the major AnNitA band migrated with an apparent mass of 58 kDa, which corresponds to an actual mass of 32 kDa, close to the mass of 33.6 kDa predicted from the amino acid sequence. Fainter but higher-molecular-mass bands in this lane probably correspond to dimeric and trimeric intermediates formed upon SDS denaturation.

Western blots of *A. nidulans* membranes following BN-PAGE. No reaction to the anti-V5 antibody was observed with strain T110, which expresses wild-type AnNitA without the V5 tag (Fig. 4, lane 1). However, in membranes prepared from a transformant strain expressing wild-type V5-tagged AnNitA

(strain T600), the size of the immune-reacting band corresponded to a tetramer (lane 3). Pretreatment with 1% SDS resulted in bands of the size expected for the AnNitA monomer and dimer (lane 2). Although equal amounts of protein were loaded, the signal for the monomer/dimer is weaker than that for the tetrameric form, perhaps due to poor transfer from the higher gel concentrations under the conditions used for blotting. Nevertheless, the results show that it is possible to distinguish between different oligomeric states of the protein.

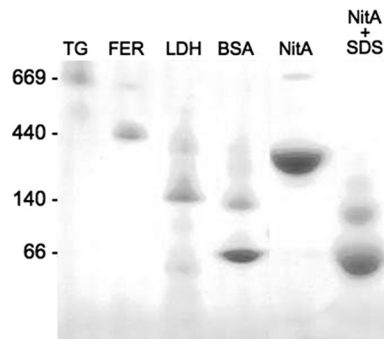


FIG. 3. Blue native gel electrophoresis of purified AnNitA. Samples (15 µg) of the *A. nidulans* AnNitA protein expressed in *P. pastoris*, solubilized in 0.016% DDM or incubated at room temperature for 30 min in 1% SDS prior to loading, were run on a 5-to-17% gradient BN-PAGE gel along with 5 µg each of molecular size markers thyroglobulin (TG), ferritin (FER), lactate dehydrogenase (LDH), and bovine serum albumin (BSA), the sizes of which are shown on the left. Following electrophoresis, the gel was destained to remove residual Coomassie stain.

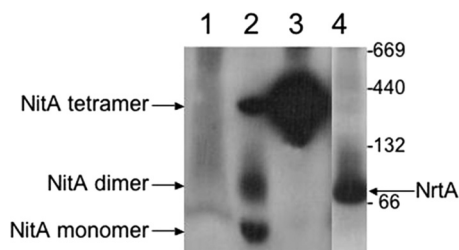


FIG. 4. Western blot of proteins from crude membrane preparations of *Aspergillus nidulans* separated on BN-PAGE gels. Proteins from crude membranes were run in 5-to-17% gradient BN-PAGE gels and blotted onto a PVDF membrane, and protein was detected by using anti-V5 antibody and ECL Plus reagents. Lane 1 contains around 50 μ g of protein from strain T110 (wild-type AnNitA without a V5 tag). For lanes 2 and 3, membranes were prepared from a transformant strain, T600, expressing wild-type V5-tagged AnNitA. Both lanes contain around 20 μ g of protein, but the sample in lane 2 was exposed to 1% SDS for 15 min prior to loading. Lane 4 contains 50 μ g of protein from *A. nidulans* strain T454 expressing the V5-tagged, nitrate/nitrite transporter AnNrtA for size comparisons. The exposure time for lanes 1 to 3 was approximately 10 times longer than that for lane 4 to ensure that no signal was visible in lane 1 and in order to see the bands in lane 2 clearly. Molecular masses of soluble protein standards (in kilodaltons) are shown. The masses of the membrane proteins were calculated according to a formula described previously by Heuberger and colleagues (11).

Conserved asparagine residues and models of AnNitA. In an alignment of 643 FNT protein sequences generated in the Pfam database (accession number PF01226; <http://pfam.sanger.ac.uk>), residue N122 in Tm 3 and N246 in Tm 6 were present in 100% of sequences, while N173 in Tm 4 and N214 in Tm 5b were represented in more than 80% of sequences (9). No highly conserved arginine residues (which are involved in substrate binding in the nitrate/nitrite transporter AnNrtA) were observed in Tms. A secondary structure model of the *A. nidulans* 33.6-kDa AnNitA monomer based on an alignment with EcFocA (PDB accession number 3KCU) of known structure is shown in Fig. 5A, with the asparagine residues highlighted. The model shows the six Tms, including the broken Tm 2a and Tm 2b as well as Tm 5a and Tm 5b, joined by short segments termed the Ω and S loops, respectively (38). The dashed lines represent the approximate extent of the lipid bilayer, and the position of the so-called P helix is shown on the outside of the membrane. Figure 5B is a representation of the 3D monomer structure viewed from the plane of the membrane, and Fig. 5C shows the positions of the conserved asparagine residues and their proximity to the Ω and S loops within the 3D model. The Tms are rainbow colored as in the 2D model.

Asparagine residue replacements. Our previous mutagenesis studies of AnNrtA have shown that an asparagine residue is intimately associated with nitrate binding (35), and so the presence of highly conserved asparagine residues in predicted Tm regions of the FNT family is intriguing. Consequently, these four highly conserved polar asparagine residues, i.e., N122 (Tm 3), N173 (Tm 4), N214 (Tm 5), and N246 (Tm 6), were altered (in an *nrtA nrtB* mutant background) to determine if such changes affected the ability to grow on nitrite as the sole source of nitrogen. As a general strategy, residues were altered to Q (polar with a bulkier side chain than that of N), S (polar with a less bulky side chain), K (positively charged with a

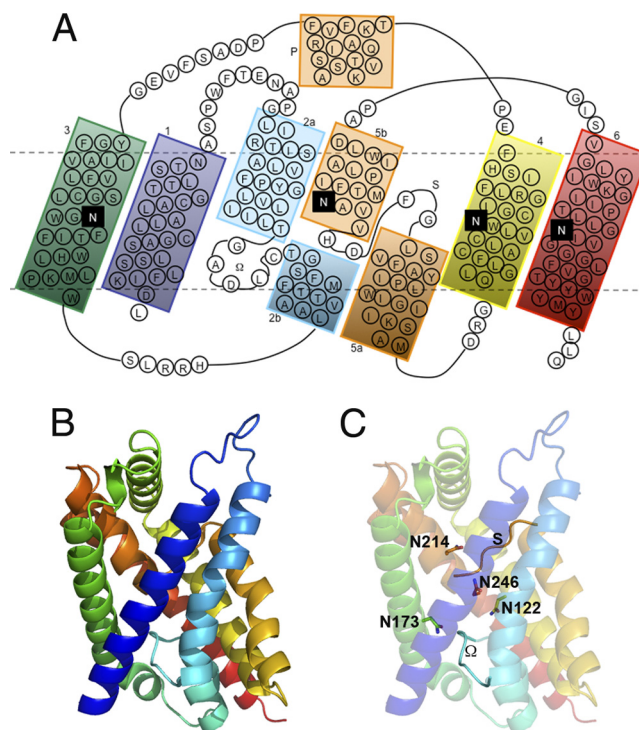


FIG. 5. Secondary and tertiary structure models of AnNitA. (A) Secondary structure model generated by comparison to the crystal structure of EcFocA (PDB accession number 3KCU). The N-terminal 28 residues and the C-terminal 45 residues were not included in the model. Tms are rainbow colored from blue (N terminal) to red (C terminal). A comparison of 643 amino acid sequences in the Pfam protein families database (9) was examined to identify the highly conserved asparagine residues outlined in black: N122 in Tm 3, N173 in Tm 4, N214 in Tm 5b, and N246 in Tm 6. (B and C) Tertiary structure model of the AnNitA monomer viewed from the plane of the membrane (B) and the same tertiary structure model showing the relative positions of the conserved asparagine residues as well as the Ω and S loops between Tm 2a/2b and Tm 5a/5b, respectively (C).

bulkier side chain than that of N), and D (negatively charged with a side chain similar to that of N). In addition, amino acid replacements of two nonconserved residues, L127 (Tm 2) with V and C177 (Tm 4) with T, were made as controls to ensure that a change in a Tm residue *per se* did not result in a loss of function. The growths of the L127V and C177T mutants were similar to that of the AnNitA wild-type strain (T600), as were expression levels, judging by Western blot analyses (data not shown).

In order to evaluate the effects of asparagine substitutions on the growth of *A. nidulans* strains, fungi were grown at several nitrite concentrations, including 250 μ M, 500 μ M, 1 mM, 1.5 mM, and 2.0 mM. Generally, relative growths with the different nitrite concentrations were similar; strains T600 (expressing AnNitA) and T26 (in the absence of AnNitA) represented the extremes of high growth rates and virtually no growth, respectively (Fig. 6A, showing data for 2 mM nitrite in cells grown at 37°C). No temperature sensitivity or cryosensitivity differences were observed for any of the asparagine-altered mutants; i.e., mutants had approximately similar growth phenotypes whether assessed at 37°C or 25°C. Alterations of residues N122 or N246 to Q, S, K, or D were not

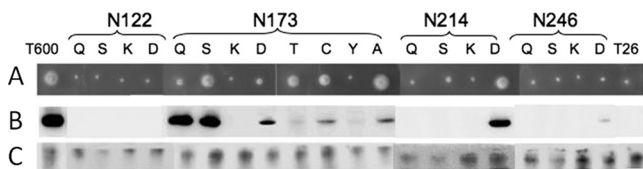


FIG. 6. Growth and Western analysis of AnNitA asparagine replacement mutants. (A) Growth phenotypes of missense mutant strains compared with strain T600 (expressing wild-type AnNitA) and strain T26 (in the absence of AnNitA) were assessed after 3 days at 37°C on minimal medium containing 2 mM nitrite as the sole nitrogen source. All strains are in an *nrtA747 nrtB110* background. (B) Crude membrane preparations from cells grown for around 5 h at 37°C with urea as the sole nitrogen source and induced with nitrite for a further 3 h at 37°C were solubilized in 1% DDM, and proteins were separated by BN-PAGE and blotted onto PVDF membranes for immunodetection with HRP-conjugated anti-V5 antibody. (C) Blots were washed in stripping buffer, and immunodetection was repeated by using the cross-reacting *S. cerevisiae* Pma1 H⁺-ATPase antibody to assess the approximate equality of protein loading and transfer.

tolerated, as judged by the absence of growth of the resultant mutant strains (similar to strain T26) on 2 mM nitrite as the sole source of nitrogen (Fig. 6A). Western blots of BN gels detected no V5-tagged AnNitA protein in membrane preparations from the N122 mutant strains or the N246Q, N246S, and N246K mutants, although the N246D protein was detected albeit at a lower level than that of the wild type (Fig. 6B). To circumvent the potential problem of transfer from the high gel concentration of the BN gradient gel, and in order to check whether low levels of monomer might be detectable, 10% SDS-PAGE gels of the same membrane preparations were subjected to Western blotting (S. E. Unkles, unpublished data). The presence of the monomer under denaturing conditions correlated well with the expression of the oligomer. After a long exposure of the blot, the AnNitA monomer was barely detectable in the N122 mutants or the N246Q, N246S, and N246K mutants, while the monomer was clearly detectable in the N246D mutant at a lower level than that for the wild type.

Modifications of N173 to Q, K, or D resulted in growth levels similar to that of the *nitA* deletion strain, whereas an alteration to S resulted in relatively higher levels of growth. Therefore, a further series of changes of N173 to the other polar residues T (slightly larger than S), C (intermediate size between S and T), and Y (bulky aromatic) was undertaken. Finally, N173 was changed to the smaller (than N) nonpolar A (which resembles S but without the hydroxyl group). The change to A provided growth similar to those of the N173S, N173T, and N173C mutants, exhibiting poorer but nevertheless significant growth, while alterations to the aromatic Y residue did not allow growth. Western blots of BN-PAGE gels showed that the N173Q and N173S mutant proteins were expressed at levels similar to those of the wild type; N173C, N173D, and N173A levels were reduced; N173T and N173Y levels were barely detectable, and N173K levels were undetectable. The observation that the growths of the N173A, N173C, and N173T mutants were similar to that of the wild type but that the protein levels were considerably lower suggests that these mutant proteins, while functional *in vivo*, are somewhat labile during membrane purification. As observed for the N122 and N246 mutants, the levels of the monomer detected under

denaturing conditions in N173 mutants mirrored those obtained with BN-PAGE (Unkles, unpublished).

Changes of N214 to Q or K were not tolerated, but poor growth was observed for the N214S mutant and approached wild-type levels of growth for the N214D mutant. The expression of the N214D protein was of a level comparable to that of the wild type in Western blots of BN-PAGE gels, but the protein was barely detectable in membranes from the N214Q and N214S mutants and undetectable in membranes from the N214K mutant. Western blots of membrane preparations from both the N173 and N214 mutants run on SDS-PAGE gels generally reflected the results obtained by BN-PAGE.

¹⁵N-nitrite tracer influx was assayed for strains T600 and T26 to establish points of reference and for amino acid replacement strains that exhibited some growth, i.e., the N173A, N173S, N214D, and N214S strains, in order to verify that any growth effects of asparagine substitutions were being exerted as a consequence of altered nitrite uptake rather than by pleiotropic effects associated with the altered amino acid composition of the AnNitA mutants. Compared to T600 and T26, which generated hyperbolic and linear concentration plots, respectively (Fig. 2A), the N173A, N173S, and N214S mutants gave fluxes that responded to the nitrite concentration in a linear rather than a hyperbolic fashion. Flux at 250 μM nitrite for the N214D strain was significantly higher than that for T26 but lower than that for T600. Fluxes for the N173A, N173S, and N214S strains were intermediate between T26 and the N214D strain.

DISCUSSION

The observation that strain T600 (*nrtA747 nrtB110*), lacking nitrate transport, could still maintain growth on nitrite suggested the activity of a discrete nitrite transporter that is incapable of transporting nitrate (40). A similar conclusion was arrived at from previous studies of nitrite uptake by *Hansenula polymorpha* (17) and *A. nidulans* (22). However, another possibility is that the conjugate acid of nitrite (nitrous acid), rather than the nitrite anion *per se*, might permeate the cell membrane to support growth. For example, it was suggested previously that nitrite entry into pea root plastids was done by passive diffusion, based upon rates of ¹⁵NO₂⁻ entry (2). We made use of ¹⁵N-labeled nitrite to explore this question with *A. nidulans* by incubating strain T26 (i.e., the *nrtA747 nrtB110 nitA26* triple deletion mutant) in medium that nominally contained 250 μM nitrite and varied the nitrous acid concentration by altering the ambient pH (Fig. 1). As anticipated, tracer accumulation increased logarithmically as ambient pH values were decreased from pH 8.5 to 3.5 ($r^2 = 0.95$), consistent with increasing nitrous acid permeation as the pH declined. This raises the interesting conjecture that even without the AnNrtA and AnNrtB (nitrate/nitrite) transporters and AnNitA, significant quantities of nitrite (actually nitrous acid) might permeate the plasma membrane at a low pH. While most soils have pH values closer to pH 5 and 6, lower pH values are common in forest soils. However, at more typical soil pH values, ¹⁵N-nitrite influx in T26 mycelium was low compared to the flux of nitrite through the AnNitA transporter in strain T600 expressing wild-type AnNitA (in the *nrtA747 nrtB110* double deletion background). Furthermore, the fluxes showed linear concen-

tration dependence in T26, with no indication of saturation as the external nitrite concentration was varied from 10 to 200 μM . Thus, unless we were to operate at pH values of less than pH 5.5, there is little nitrous acid permeation. Typically, ^{13}N -nitrite flux analyses and growth tests were conducted at pH 6.5 or 7.5, at which pH nitrous acid concentrations are <1% or <0.1%, respectively, of the nitrite concentration. It is therefore likely, except at unrealistically high nitrite concentrations, that nitrous acid is a minor permeating species. Comparisons of influx at 250 μM to values at 2.0 mM for various strains using T600 as the point of reference demonstrated that the reduction of influx associated with the deletion of the *nitA* gene or amino acid modification was consistently much lower at 2 mM than at 250 μM nitrite. This observation is consistent with increasing nitrous acid permeation at elevated nitrite concentrations. However, it is highly unlikely that nitrite concentrations would reach mM levels under natural conditions. Additional evidence that it is nitrite and not nitrous acid that is transported at higher pH values comes from mutant growth tests. Strain T26 (*nrtA747 nrtB110 nitA26*) failed to grow on nitrite (at all concentrations up to and including 2 mM) as the sole source of nitrogen at pH 7.5, whereas there was some growth at lower pH values. This provides evidence that the nitrous acid permeation, although detectable by use of ^{13}N -nitrite and significant at 2.0 mM, was insufficient to sustain the normal growth of *A. nidulans*. The importance of the AnNitA transporter for nitrite entry is also demonstrated by the restoration of saturable influx following the knock-in transformation of the T26 triple mutant with wild-type *nitA*. Q_{10} estimates for high-affinity nitrite influx gave clear evidence of a strong metabolic dependence, while the absence of any reduction of nitrite influx in the presence of a considerable excess of formate suggests that NitA is a nitrite transporter with no capacity for formate transport. Consistent with this observation was the finding that formate uptake by T26 was not reduced compared to the uptake by T600.

The data presented in Fig. 2A reveal that strain T600 exhibited typical hyperbolic kinetics for ^{13}N -nitrite influx, with V_{\max} and K_m values of $212 \pm 11 \text{ nmol mg}^{-1} \text{ DW h}^{-1}$ and $35 \pm 2.5 \mu\text{M}$, respectively. Thus, although this strain is incapable of growth on nitrate or of ^{13}N -nitrate influx, it is capable of growth on nitrite and saturable nitrite influx. In contrast, T26, lacking AnNitA, exhibited linear fluxes of substantially lower magnitudes (Fig. 2A), and a knock-in transformation of this strain with the wild-type *nitA* gene restored hyperbolic kinetics (Fig. 2B). Because of the oligomeric nature of AnNitA, we examined the kinetics of ^{13}N -nitrite influx down to a concentration of 0.25 μM in order to explore sigmoidal kinetics that might indicate cooperative interactions among the four subunits. As shown in Fig. 2A, no deviation from hyperbolic kinetics was apparent. Using ^{14}N -nitrite net uptake values reported in a previous study (40), we reported V_{\max} and K_m values of $168 \pm 21 \text{ nmol mg}^{-1} \text{ DW h}^{-1}$ and $4.2 \pm 1 \mu\text{M}$, respectively. The lower K_m value in the previous study is probably the result of several differences in protocols. First, $^{13}\text{NO}_2^-$ provides measurements of unidirectional influx rather than net flux (influx minus efflux). Second, in the previous study, the induction of mycelia was achieved by 100 min of exposure to 10 mM nitrate, while in the present study, mycelia were induced by 5 mM nitrite for 3 h. The net nitrite uptake following

induction by nitrite resulted in a substantially higher K_m than that for nitrate induction (data not shown). The accumulation of cytoplasmic nitrite by the latter methodology may account for this effect upon K_m values, as was observed previously for effects of accumulated K^+ and NH_4^+ on the influxes of K^+ and NH_4^+ , respectively (39). Even higher K_m values (640 μM) were reported in a previous study of nitrite uptake by *A. nidulans* (22). These differences indicate the sensitivity of measured K_m values to assay conditions; unlike enzyme assays, wherein conditions are highly regulated and reproducible, K_m values for transport processes are a measure of a physiological status and highly sensitive to growth conditions.

Preliminary work had shown that the change of two nonconserved Tm residues (i.e., L127V and C177T) *per se* had no apparent effect on either the growth phenotype or protein expression. The four conserved asparagine residues were chosen for mutagenesis because these were identified from alignments as being the only highly conserved, noncharged, polar residues within Tms of the formate-nitrate transporters. Additionally, asparagine is interesting because of its propensity to act as a hydrogen bond donor or acceptor and, hence, the potential for the side-chain amide group to coordinate either the nitrogen or the oxygen atoms within nitrite. However, in the light of the published crystal structures of the three formate channels, it appears that the function of these asparagine residues is primarily to constrain or govern the flexibility of the Ω and S loops through networks of hydrogen bonds (15, 38, 41). The disruption of this function may be responsible for the observed lack of expression in many of the mutants in this study.

A further function may exist for N173, whose counterpart in VcFocA was proposed, in addition, to interact directly via a hydrogen bond to the substrate formate following the movement of the Ω loop as part of the hypothesized gating mechanism (38). In terms of the growth phenotype, replacements of N173 by residues with a smaller side-chain bulk permitted the growth of mutants on 2 mM nitrite as the sole nitrogen source regardless of whether the replacement residue was polar (S, C, or T), or nonpolar (A), although rates of growth at 250 and 500 μM nitrite were significantly lower than that of T600. The replacement of N173 by the charged residue (D) resulted in only marginal growth at 2.0 mM nitrite. Mutants with a substitution to the bulkier amide side chain (Q) showed marginal growth, while mutants with changes of N173 to yet bulkier residues (K and Y) were incapable of growth on nitrite. The results of phenotypic tests were reflected in protein expression in that smaller residues tended to have expression levels that were somewhat reduced (D, T, C, or A) or close to those of the wild type (Q or S), while much larger residues (K and Y) showed very poor or no protein expression. The results illustrate that asparagine at position 173, although not essential, influences nitrite transport. N173 appears to reside in a region of the protein at which there is a constraint of space, and so residues bulkier than asparagine reduce or prevent protein expression and/or activity. Indeed, N173 resides in a region where in FocA proteins there is a "slit" or constriction of the channel through which the substrate must pass (38, 41). The change from hyperbolic to linear fluxes in the N173 mutants that grew on nitrite suggests that a reduction in the side-chain volume at this position disrupts normal fluxes of nitrite through

the transporter, perhaps by allowing the nitrite to slip through the constriction. N173 may therefore act as part of a gate or barrier within the transporter which regulates the flux of nitrite through the translocation pathway.

The introduction of a charged residue into a Tm is thermodynamically unfavorable and often perturbs protein expression. However, N214 can be replaced by aspartate, with little effect on growth or protein expression, and the replacement of N173 and N246 with D, while adversely affecting growth on nitrite, nevertheless permitted some protein expression. This finding suggests that the negative charges introduced at these positions are neutralized, probably via hydrogen bond networks with neighboring residues.

While the replacement of N214 with the negatively charged aspartate was tolerated well in terms of the growth of the mutant strain and protein expression, other substitutions reduced (S) or completely abolished (Q or K) the ability of mutants to grow on nitrite and severely disrupted protein expression. An asparagine-to-aspartate change could be regarded as very conservative, particularly if N214 is involved as a hydrogen bond acceptor, but it might be expected that glutamine would substitute well in that situation. The finding that there is no activity in the N214Q mutant (as determined by growth on nitrite) and, more particularly, no protein expression suggests severe restrictions on space at that residue position such that even a moderate increase in side-chain bulk is not tolerated. The suggestion was made previously that in EcFocA, hydrogen bonding was possible between the residue equivalent to N214 and the substrate (41), and therefore, a replacement aspartate residue with its similar bulk and ability to accept hydrogen bonds could still permit interactions with nitrite and the observed activity.

None of the substitutions of N122 or N246 tested (D, K, Q, or S) allowed the growth of the corresponding mutant on nitrite, and although some protein expression was detected for the N246D mutant, all the other mutants failed to produce protein. It would appear that asparagine at positions 122 and 246 is important for the correct folding of the protein and, hence, protein expression, but it is not possible to deduce from these results if they also serve a role in the passage of nitrite.

The BN gel analysis as well as a previous study by size-exclusion chromatography (1) appeared to indicate that the AnNitA protein is a tetramer. Crystal structures of the FNT family formate channels, however, show that these proteins are pentameric. Given the experimental error inherent in both PAGE and chromatographic estimations of protein size, it is likely that AnNitA is similarly pentameric. Nevertheless, proteins with a similar 3D fold, i.e., the aquaporins, are tetramers (10, 29). Also, there are some differences in primary amino acid sequences of biochemically verified formate versus nitrite transporters, notably in the length of the loop between Tm 5 and Tm 6 to 20 residues in VcFocA, versus the predicted 5 residues in AnNitA, for example. Therefore, a definitive answer to the quaternary organization of FNT nitrite transporters awaits a crystal structure. Finally, however, as conjectured previously by Waight et al. (38) for VcFocA and regardless of the quaternary structure, the absence of any sigmoidal kinetics suggests that cooperativity is absent among the protein monomers.

ACKNOWLEDGMENTS

This work was supported by grants to A.D.M.G. from NSERC and to S.E.U. and J.R.K. from the BBSRC. V.F.S. acknowledges travel funds from the Maitland Ramsey Fund (St. Andrews, United Kingdom). J.R.K. acknowledges travel funds from the Carnegie Trust (Scotland, United Kingdom).

We gratefully acknowledge the support of TRIUMF staff in providing ^{15}N .

REFERENCES

1. Beckham, K. S. H., J. A. Potter, and S. E. Unkles. 2010. Formate-nitrite transporters: optimisation of expression, purification and analysis of prokaryotic and eukaryotic representatives. *Protein Expr. Purif.* **71**:184–189.
2. Bowsher, C. G., et al. 2007. The effect of Glc6P uptake and its subsequent oxidation within pea root plastids on nitrite reduction and glutamate synthesis. *J. Exp. Bot.* **58**:1109–1118.
3. Clegg, S., Y. Feng, L. Griffiths, and J. A. Cole. 2002. The roles of the polytopic membrane proteins NarK, NarU and NirC in *Escherichia coli* K-12: two nitrate and three nitrite transporters. *Mol. Microbiol.* **44**:143–155.
4. Clutterbuck, A. J. 1974. *Aspergillus nidulans*, p. 447–510. In R. C. King (ed.), *Handbook of genetics*, vol. 1. Plenum Press, New York, NY.
5. Cove, D. J. 1966. Studies on temperature-sensitive mutants affecting the assimilatory nitrate reductase of *Aspergillus nidulans*. *Biochim. Biophys. Acta* **113**:51–56.
6. DeLano, W. L. 2002. The PYMOL user's manual. DeLano Scientific, San Carlos, CA.
7. Falke, D., et al. 2010. Unexpected oligomeric structure of the FocA formate channel of *Escherichia coli*: a paradigm for the formate-nitrite transporter family of integral membrane proteins. *FEMS Microbiol. Lett.* **303**:69–75.
8. Fernandez, E., and A. Galvan. 2008. Nitrate assimilation in *Chlamydomonas*. *Eukaryot. Cell* **7**:555–559.
9. Finn, R. D., et al. 2008. The Pfam protein families database. *Nucleic Acids Res.* **36**:D281–D288.
10. Fu, D., et al. 2000. Structure of a glycerol-conducting channel and the basis for its selectivity. *Science* **290**:481–486.
11. Heuberger, E. H. M. L., L. M. Veenhoff, R. H. Duurkens, R. H. E. Friesen, and B. Poolman. 2002. Oligomeric state of membrane transport proteins analyzed with blue native electrophoresis and analytical ultracentrifugation. *J. Mol. Biol.* **317**:591–600.
12. Jia, W., and J. A. Cole. 2004. Nitrate and nitrite transport in *Escherichia coli*. *Biochem. Soc. Trans.* **33**:159–161.
13. Jia, W., N. Tovell, S. Clegg, M. Trimmer, and J. A. Cole. 2009. A single channel for nitrate uptake, nitrite export and nitrite uptake by *Escherichia coli* NarU and a role for NirC in nitrite export and uptake. *Biochem. J.* **417**:297–304.
14. Lee, R. B. 1979. The effect of nitrate on root growth of barley and maize. *New Phytol.* **83**:615–622.
15. Lü, W., et al. 2011. pH-dependent gating in a FocA formate channel. *Science* **332**:352–354.
16. Lundberg, J. O., E. Weitzberg, J. A. Cole, and N. Benjamin. 2004. Nitrate, bacteria and human health. *Nat. Rev. Microbiol.* **2**:593–602.
17. Machin, F., et al. 2004. The role of Ynt1 in nitrate and nitrite transport in the yeast *Hansenula polymorpha*. *Yeast* **21**:265–276.
18. Mariscal, V., et al. 2006. Differential regulation of the *Chlamydomonas* NarI gene family by carbon and nitrogen. *Protist* **157**:421–433.
19. McElfresh, M. W., J. C. Meeks, and N. J. Parks. 1979. The synthesis of ^{15}N -labelled nitrite of high specific activity and purity. *J. Radioanal. Chem.* **53**:337–344.
20. Needoba, J. A., D. M. Sigman, and P. J. Harrison. 2004. The mechanism of isotope fractionation during algal nitrate assimilation as illuminated by the $^{15}\text{N}/^{14}\text{N}$ of intracellular nitrate. *J. Phycol.* **40**:517–522.
21. Nelissen, B., R. de Wachter, and A. Goffeau. 1997. Classification of all putative permeases and other membrane plurispansers of the major facilitator superfamily encoded by the complete genome of *Saccharomyces cerevisiae*. *FEMS Microbiol. Rev.* **21**:113–134.
22. Pombeiro-Sponchiado, S. R., A. Rossi, S. W. Han, and N. M. Martinez-Rossi. 1993. Kinetic studies of nitrite uptake by *Aspergillus nidulans*. *Braz. J. Med. Biol. Res.* **26**:151–161.
23. Rexach, J., E. Fernandez, and A. Galvan. 2000. The *Chlamydomonas reinhardtii* NarI gene encodes a chloroplast membrane protein involved in nitrite transport. *Plant Cell* **12**:1441–1453.
24. Riach, M., and J. R. Kinghorn. 1995. Genetic transformation and vector developments in filamentous fungi, p. 209–234. In C. Bos (ed.), *Fungal genetics: principles and practice*. Wiley, London, United Kingdom.
25. Saier, M. H., Jr., et al. 1999. The major facilitator superfamily. *J. Mol. Microbiol. Biotechnol.* **1**:257–279.
26. Sali, A., and T. L. Blundell. 1993. Comparative protein modelling by satisfaction of spatial restraints. *J. Mol. Biol.* **234**:779–815.
27. Söding, J., A. Biegert, and A. N. Lupas. 2005. The HHpred interactive server

- for protein homology detection and structure prediction. *Nucleic Acids Res.* **33**:W244–W248.
28. Sugiura, M., M. N. Georgescu, and M. Takahashi. 2007. A nitrite transporter associated with nitrite uptake by higher plant chloroplasts. *Plant Cell Physiol.* **48**:1022–1035.
29. Sui, H., B. G. Han, J. K. Lee, P. Walian, and B. K. Jap. 2001. Structural basis of water-specific transport through the AQP1 water channel. *Nature* **414**:872–878.
30. Suppmann, B., and G. Sawers. 1994. Isolation and characterization of hypophosphite-resistant mutants of *Escherichia coli*: identification of the FocA protein, encoded by the pfl operon, as a putative formate transporter. *Mol. Microbiol.* **11**:965–982.
31. Szewczyk, E., et al. 2006. Fusion PCR and gene targeting in *Aspergillus nidulans*. *Nat. Protoc.* **1**:3111–3120.
32. Thompson, J. D., D. G. Higgins, and T. J. Gibson. 1994. CLUSTAL W: improving the sensitivity of progressive multiple sequence alignment through sequence weighting, position-specific gap penalties and weight matrix choice. *Nucleic Acids Res.* **22**:4673–4680.
33. Trueman, L. J., A. Richardson, and B. G. Forde. 1996. Molecular cloning of higher plant homologues of the high-affinity nitrate transporters of *Chlamydomonas reinhardtii* and *Aspergillus nidulans*. *Gene* **175**:223–231.
34. Unkles, S. E., I. S. Heck, M. V. C. L. Appleyard, and J. R. Kinghorn. 1999. Eukaryotic molybdopterin synthase. Biochemical and molecular studies of *Aspergillus nidulans* cnxG and cnxH mutants. *J. Biol. Chem.* **274**:19286–19293.
35. Unkles, S. E., et al. 2004. Two perfectly conserved arginine residues are required for substrate binding in a high-affinity nitrate transporter. *Proc. Natl. Acad. Sci. U. S. A.* **101**:17549–17554.
36. Unkles, S. E., D. Zhuo, M. Y. Siddiqi, J. R. Kinghorn, and A. D. M. Glass. 2001. Apparent genetic redundancy facilitates ecological plasticity for nitrate transport. *EMBO J.* **22**:6246–6255.
37. Vermeer, I. T. M., and J. M. S. van Maanen. 2001. Nitrate exposure and the endogenous formation of carcinogenic nitrosamines in humans. *Rev. Environ. Health* **16**:105–116.
38. Waight, B. A., J. Love, and D. N. Wang. 2010. Structure and mechanism of a pentameric formate channel. *Nat. Struct. Mol. Biol.* **17**:31–37.
39. Wang, M. Y., M. Y. Siddiqi, and M. Glass. 1996. Interactions between K^+ and NH_4^+ : effects on ion uptake by rice roots. *Plant Cell Environ.* **19**:1037–1046.
40. Wang, Y., et al. 2008. Nitrite transport is mediated by the nitrite-specific high-affinity NitA transporter and by nitrate transporters NrtA, NrtB in *Aspergillus nidulans*. *Fungal Genet. Biol.* **45**:94–102.
41. Wang, Y., et al. 2009. Structure of the formate transporter FocA reveals a pentameric aquaporin-like channel. *Nature* **462**:467–472.
42. Warrens, A. N., M. D. Jones, and R. I. Lechler. 1997. Splicing by overlap extension by PCR using asymmetric amplification: an improved technique for the generation of hybrid proteins of immunological interest. *Gene* **186**:29–35.